Biochimica et Biophysica Acta, 1065 (1991) 250–260
© 1991 Elsevier Science Publishers B.V. 0005-2736/91/$03.50
ADONIS 000527369100245H

BBAMEM 75250

Early response of cultured lepidopteran cells to exposure to δ-endotoxin from *Bacillus thuringiensis*: involvement of calcium and anionic channels *

Jean-Louis Schwartz [1], Line Garneau [2], Luke Masson [2] and Roland Brousseau [2]

[1] *Institute for Biological Sciences, National Research Council, Ottawa (Canada) and* [2] *Biotechnology Research Institute, National Research Council, Montreal (Canada)*

(Received 2 November 1990)

Key words: Ion channel; Calcium ion; Chloride; SF-9 cell; δ-Endotoxin; Fura-2; (*B. thuringiensis*)

The role of ion channels in the initial steps following exposure of SF-9 lepidopteran insect cells in culture to the δ-endotoxin CryIC from the insecticidal bacterium *Bacillus thuringiensis* was investigated using single ionic channel measurements and microspectrofluorescence of the calcium-sensitive probe fura-2. It was found that: (1) the toxin triggers an immediate rise in intracellular calcium; (2) the surge is due to calcium entering the cells via calcium channels; (3) the toxin recruits or introduces anionic channels in the cell's plasma membrane in a time-dependent manner. These channels, not seen in the absence of the toxin, are induced by toxin exposure to either side of the cell membrane. They have a conductance of 26 picosiemens (pS) and are mainly permeable to chloride. This study provides the first evidence of the primary role of calcium and chloride ions in the action of δ-endotoxin on cultured insect cells.

Introduction

Major interest in the Gram-positive bacterium, *Bacillus thuringiensis,* stems from its ability to produce a large, intracellular proteinaceous crystal during sporulation. This crystal has been shown by various investigators to be toxic to a variety of insect larvae spanning three insect orders, lepidoptera, diptera and coleoptera [1–3]. In recent years, a number of different toxin genes have been characterized and cloned from this organism. The cloned genes have been assembled into 13 different classes or subclasses based primarily on genetic data and insecticidal spectrum [3].

Although it is generally accepted that the crystal toxin exerts its effect by disrupting the ion balance of the plasma membrane of midgut cells, the exact mode of action of these entomopathic proteins remains unclear [4]. However, a number of models have appeared in the literature. A generalized model has been proposed by Knowles and Ellar [5] in which the plasma membrane is made permeable to small ions through the formation of small, non-specific pores formed after toxin interaction with a specific cell surface receptor. The pores allow a net uptake of ions into the cells, followed by water, resulting in cell swelling and eventual lysis.

A number of specific models which consider the primary toxin-membrane site of action have also been proposed. One model postulates the stimulation of Na^+ influx, K^+ efflux and the Na^+,K^+-ATPase by the δ-endotoxin [6]. Another model involves the nonspecific inhibition of the K^+-ATPase and the loss of pH regulation [7]. A K^+ channel mechanism has been suggested by Wolfersberger et al. [8], in which the primary lesion caused by the toxin is K^+ channel formation or activation. These channels would then shunt the electrogenic pump potential difference, disrupt ion gradients and pH regulation followed by eventual cell lysis. Sacchi et al. [9] examined the influence of *B. thuringiensis* toxin on Na^+ and K^+ ion gradient driven amino acid accumulation by brush border membrane vesicles of *Pieris brassicae.* Inhibition of amino acid uptake by the K^+ gradient driven cotransport but not the Na^+ provided further evidence that the ion channels may be K^+-specific. The ability of the K^+ channel blockers, barium and calcium, to inhibit the

* NRCC No. 31989.

Correspondence: J.-L. Schwartz, Institute for Biological Sciences, National Research Council, Ottawa, Ont., Canada, K1A 0R6.

short circuit current across isolated midguts of *Manduca sexta* provided additional evidence for specific K^+ ion channels [10]. However, using a system similar to Sacchi et al. [9], Wolfersberger [11] demonstrated that *B. thuringiensis* toxin was able to inhibit both the Na^+ and K^+ driven amino acid vesicles. Direct evidence for the role of ion channels has been provided by two recent studies by Knowles et al. [12] and Slatin et al. [13]. They have demonstrated that CytA, a 27 kDa cytolytic protein from *B. thuringiensis* var. *israelensis* and two different, non-cytolytic δ-endotoxins (CrylA(c) from *B. thuringiensis* var. *kurstaki* and CryIIIA from *B. thuringiensis* strain EG2158) form cation-selective channels in planar lipid bilayers at pH above 9.5.

In this study, we examined the role of ion channels in the plasma membrane of a cultured *Spodoptera frugiperda* (SF-9) lepidopteran insect cell line after exposure to the δ-endotoxin CryIC from *B. thuringiensis*. Using the patch-clamp technique [14] and microspectrofluorescence measurements [15], we demonstrate for the first time that: (1) under normal conditions, SF-9 cells display ion channel activity; (2) when exposed to a sublethal dose of purified trypsin-activated CryIC toxin, there is an immediate, non-toxic calcium influx in the cells followed by the activation of anion-selective channels that are either endogenous or formed de novo by the toxin in the plasma membrane of these toxin-sensitive cells.

Materials and Methods

Chemicals and solutions

Cell culture media i.e. Grace medium, Yeastolate and Lactalbumin were purchased from GIBCO BRL, Gaithersburg, MD. Trypan blue, Pipes (1,4-piperazinediethanesulfonic acid) and CAPS (3-[cyclohexylamino]-1-propane-sulfonic acid) were purchased from Sigma, St Louis, MO. Renografin was obtained from Squibb, Montreal, Que. Fura-2/AM, ionomycin (calcium salt) and D-600 (methoxyverapamil) were purchased from Calbiochem, La Jolla, CA. Pluronic F-127 was obtained from Molecular Probes (Eugene, OR). EGTA (ethylene glycol-*O*,*O*'-bis(2-aminoethyl) *N*,*N*,*N*',*N*'-tetraacetic acid) was purchased from Fluka (Caledon Lab., Georgetown, Ont.).

In the cell-attached configuration of the patch-clamp technique (see below), the normal pipette-filling solution contained (mM): 135 KCl, 2.0 $MgCl_2$, 10.0 Pipes and 2.0 EGTA. The normal bath solution (NBS) contained (mM): 130 NaCl, 5.0 KCl, 1.2 $CaCl_2$, 2.0 $MgCl_2$, 10.0 Pipes, and 5.0 glucose. In the inside-out configuration of the patch-clamp technique, the pipette-filling solution was the same as above. It was also used in the bath. For selectivity studies, chloride ions in the pipette were partly or completely replaced by aspartate, acetate or sulfate ions. In some experiments, potassium was replaced by choline. The pH of all solutions was adjusted to 6.3 and their osmolality was brought to 380 mosmol/kg with sucrose.

Cells

Spodoptera frugiperda (SF-9) cells (lepidoptera, fall armyworm) were seeded into spinner flasks to an initial density of about $1.0 \cdot 10^6$ cells/ml (in Grace medium supplemented with Yeastolate, Lactalbumin hydrolysate and 10% fetal bovine serum) and incubated at 27 °C with constant stirring at 50–100 revolutions/min. 30 min before use, cells were plated on circular No. 1 glass coverslips.

Toxin purification

Escherichia coli (HB101) containing the cloned CryIC gene from *B. thuringiensis* var. *aizawai* was grown in 1.5 liters L-broth containing 100 mg/l of ampicillin for two days at 37 °C. The cells were harvested, lysed by passage through a french pressure cell at $7.6 \cdot 10^7$ Pascals (P) internal pressure and the protoxin purified in the form of insoluble inclusion bodies. Renografin, a mixture of 66% meglumine diatrizoate and 10% sodium diatrizoate, was utilized to further purify the inclusion bodies as described elsewhere [16]. Activated recombinant CryIC toxin was purified by solubilization of inclusion bodies in 10 mM NaOH followed by the addition of trypsin to a 1% (w/v) final concentration. The mixture was left for 5 to 12 h at ambient temperature followed by centrifugation at $2 \cdot 10^5 \times g$ for 2 h at 20 °C. Solid ammonium sulfate was added to the supernatant to 45% saturation, stirred at 4 °C for 30 min and the precipitate harvested and dialyzed against 50 mM CAPS buffer (pH 11). The 60 kDa toxin was further purified by FPLC. In some experiments, we used trypsin activated CryIC toxin isolated from *B. thuringiensis* var. *entomocidus* crystals. All protein concentrations were determined by the protein-dye method of Bradford [17], using bovine serum albumin as a standard.

Toxin doses

The cytolytic effect of the CryIC δ-endotoxin was studied in separate experiments performed on plated SF-9 cells incubated in NBS medium and exposed for 140 min to various concentrations of the toxin (from 1.75 mg/l to 80 mg/l). Trypan blue (0.1%: w/v) was added 3 min after the beginning of the treatment. The number of cells taking up the stain were counted every 5 min. The cytolytic effect was dose- and time-dependent. The dose-response curve at time 20 min provided a 50% effective dose (ED_{50}) of 40 μg/ml. The stock solution of toxin was diluted in distilled water and used at this dose (40 μg/ml) in all patch-clamp and fluorescence experiments. In control patch-clamp and fluorescence experiments, it was found that the same volume

of water, but without the toxin, had no effect on SF-9 cells.

Intracellular calcium measurements

Intracellular calcium concentrations were determined by fluorescence measurement of the calcium-sensitive indicator fura-2. SF-9 cells were loaded at room temperature for 30 min using 2 μM of fura-2/AM in NBS. Fura-2/AM is a membrane-permeant, calcium-insensitive ester of the calcium probe fura-2. After three washes in fura-free NBS, the cells were postincubated for 5 to 30 min in NBS at room temperature, to insure full hydrolysis of the fura-2 ester. This was verified by running excitation spectra between 320 and 420 nm at various times during the postincubation period. They were monophasic and peaked around 365 nm. Experiments were conducted at room temperature on single cells or small groups of 5–9 cells in a custom-made coverslip holder fitted to the stage of a Zeiss IM inverted microscope (Carl Zeiss Canada, Don Mills, Ont.) coupled to a CM3 cation measurement spectrofluorometer (Spex Inc., Newark, NJ). Measurements were performed using 350 and 380 nm excitation wavelengths alternating at a frequency of 1 Hz. The sample was illuminated through a 40X-epifluorescence objective (UVFL40, N.A. 0.85, Olympus Optical Co., Tokyo). The emitted light, after collection by the same objective, was passed through a 505 nm interference filter (10 nm bandwidth) and its intensity was recorded by a photon counter detector mounted on the microscope. Background fluorescence was subtracted from the raw data corrected for lamp intensity fluctuations. Dye leakage, as determined by loss of fluorescence over a period of 30 min, was undetectable at both excitation wavelengths with the excitation monochromator slits set at 0.5 mm.

The ratios of the fluorescence intensities at the two excitation wavelengths were then converted into an estimate of ionized intracellular calcium concentration by use of the following formula [18]:

$$[Ca^{2+}]_i = K_d \cdot (F_{min}/F_{max}) \cdot (R - R_{min})/(R_{max} - R)$$

where R, R_{min} and R_{max} are the fluorescence ratios recorded during the experiment (R) and during calibration tests on unlysed cells using 4 μM ionomycin in NBS (R_{max}), followed by 10 mM EGTA addition at pH 8.2 (R_{min}). F_{max} and F_{min} are the corresponding fluorescence intensities for the 380 nm excitation and K_d is the fura-2 dissociation constant at room temperature (135 nM).

Electrophysiology

Patch-clamp experiments were performed in the cell-attached and inside-out configurations. Patch pipettes (Pyrex 7740; 1.5 mm outside diameter; Corning Glass, Corning, NY) had resistances of 2 to 4 megohms when filled with the potassium-rich pipette solution. The seal resistances were in excess of 4 gigohms. Experiments were performed at room temperature (21–23 °C).

Single-channel currents were recorded with an Axopatch 1D patch-clamp amplifier (Axon Instruments, Burlingame, CA). Currents were filtered at 1 kHz and stored on videotape using a digital data recorder (VR-100A, Instrutech Corporation, Elmont, NY). They were played back and filtered at 400 Hz by an analog, 8-pole Bessel filter (Frequency Devices, Haverhill, MA). They were then digitized (Labmaster TL-1, Axon Instruments, Burlingame, CA) and analyzed using pClamp software (Axon Instruments, Burlingame, CA) on a personal computer.

Inward currents (i.e., currents flowing through the membrane patch from the pipette to the interior of the cell, in the cell-attached configuration, or to the bath, in the inside-out configuration) are shown as downward deflections in the figures. The direction of current flow corresponds to cation movement (anions move in the opposite direction).

Results

Intracellular calcium concentration

The intracellular calcium concentration in SF-9 cells was calculated from measured fluorescence ratios as described in Materials and Methods and was found to be 38.3 ± 3.9 nM in NBS (mean ± S.E., 12 experiments). In one single-cell experiment, the fluorescence ratio increased from 1.7 to 11.4 when the cell was treated with ionomycin in NBS and decreased to less than 1.4 upon application of EGTA in NBS (Fig. 1A), corresponding to intracellular calcium concentrations in excess of 2 μM and less than 30 nM, respectively. In the presence of δ-endotoxin, at the same dose as that used for electrophysiological experiments, a rapid rise of the fluorescence ratio was observed (Figs. 1B, 1C, 1D and 1F). The response was immediate (within 10–15 s). It displayed a fast rising phase followed by a sustained phase that lasted for several minutes (Fig. 1B). The intracellular calcium concentration was evaluated to be between 750 and 900 nM (average of seven experiments). These submicromolar concentrations of calcium had no noticeable cyototoxic effect, since the cells did not take up Trypan blue at the end of the experiments. The response to the toxin appeared to depend on extracellular calcium, as it was suppressed by addition of EGTA in the bath (Fig. 1C). Furthermore, cobalt and D-600 reversed the action of the toxin, although less rapidly in the latter case, indicating that the calcium rise was mainly due to a calcium influx through calcium channels (Figs. 1D and 1F). When the

cells were pretreated with cobalt, the toxin did not elicit any response (Fig. 1E). In other experiments performed in the absence of the toxin (results not shown), it was found that, when the cells were depolarized by raising the concentration of potassium in the bath to 45 mM, the intracellular level of calcium also increased, although to a lesser level. These depolarizing experiments and the calcium channel blocker experiments reported above suggest that SF-9 cells possess endogenous voltage-dependent calcium channels.

Intrinsic channels in SF-9 cells

In the cell-attached configuration of the patch-clamp technique, single channel activity was seldom observed in our experimental conditions. However, when channel openings took place, i.e., when discrete current jumps were seen, they usually occurred immediately after the seal formation between the glass pipette and the cell surface, and the channel activity tended to run down within minutes. Long openings alternated with long closures (Fig. 2A). Fast closures (i.e. flickering) were also seen when the channel was open, indicative of the presence of at least two distinct closed states, as revealed by time-histogram analysis (Fig. 2C). The conductance of this channel was obtained by plotting the current measured during single-channel openings vs. voltage, at various pipette voltage levels (Fig. 2B). It was 15 pS (two experiments). The reversal potential V_r, corresponding to the pipette voltage for which the channel current was zero, was 10 mV. The channel did not appear to be voltage-dependent, i.e., its mean open time did not depend on applied pipette voltage. When potassium was replaced by choline in the bath, both the conductance and the zero-current pipette voltage remained unchanged, demonstrating that it is not a potassium channel.

Channel activity in the presence of the δ-endotoxin

Single-channel activity was observed in SF-9 cells in the presence of δ-endotoxin at an ED_{50} dose. The results reported here were obtained from cells that had not lysed at the end of the experiments (31 experiments).

After seal formation using the cell-attached configuration in the normal bath solution, the toxin was added directly to the bath. In some instances, thirty seconds to 10 minutes later, an alternance of long openings and long closures of a single channel could be seen (Fig.

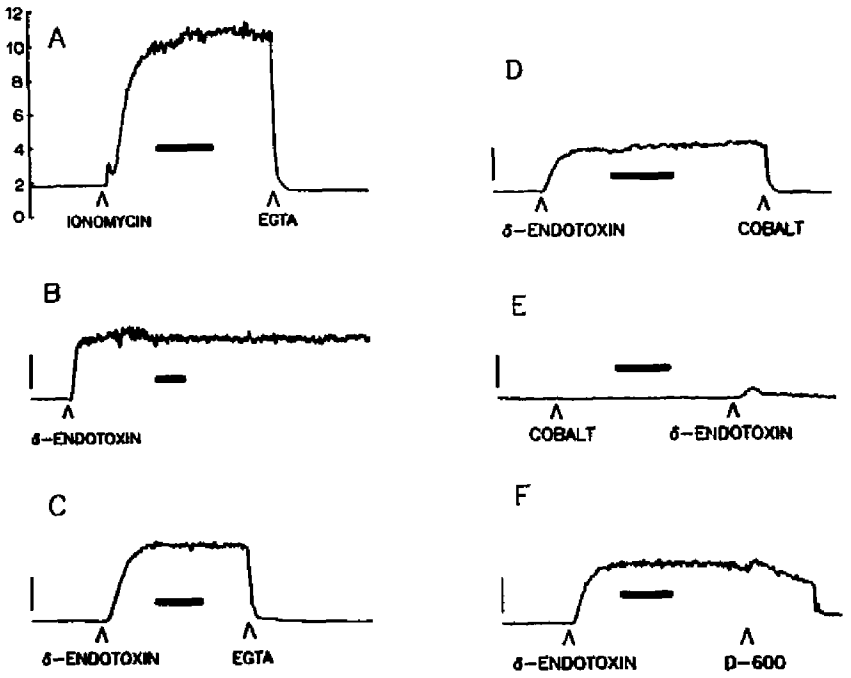

Fig. 1. Effects of δ-endotoxin on SF-9 intracellular Ca^{2+} concentration. (A) Response of a single SF-9 cell bathed in NBS to 4 μM ionomycin followed by the addition of 10 mM EGTA at pH 8.2. Vertical scale: fluorescence ratio (F_{350nm} / F_{380nm}). Horizontal bar: 50 s. (B) Sustained rise in intracellular calcium upon addition of toxin to the bath (group of seven cells). Vertical bar: 2 units of fluorescence ratio. Horizontal bar: 50 s. (C) The toxin response is suppressed when EGTA (10 mM) is added to the bath (group of nine cells). Scale bars: as in Fig. 1B. (D) Cobalt ions (5 mM) block the toxin-induced influx of calcium (group of nine cells). Scale bars: as in Fig. 1B. (E) In the presence of cobalt, there is no significant change in Ca_i^{2+} levels upon addition of the toxin (group of eight cells). Scale bars: as in Fig. 1B. (F) The calcium channel blocker D-600 (100 μM suppresses the response to the toxin (group of five cells). Note that it took almost 2 min for the complete return to baseline. Scale bars: as in Fig. 1B.

3A, top trace). The conductance and the kinetic properties of this small channel were similar to those of the channel occasionally observed in the absence of the toxin, indicating that it might be an endogenous channel. However, it cannot be excluded that the toxin was partly responsible for its recruitment. This channel, in most cases, became inactive after a few minutes, but a larger channel, with a very different kinetic behaviour, was always observed within 10 min following toxin treatment (Fig. 3, next traces). The time spent in the closed state of this second type of channel was progressively reduced and additional discrete channel opening levels could be seen. This increase in channel activity, shown as the mean open probability of N channels plotted against time (Fig. 3C), continued to the point where individual levels could no longer be resolved. The large channel appears to be related to toxin action. Identical channel activity was recorded when potassium was replaced by choline in the pipette (Fig. 3B), indicating that the inward currents observed (positive currents flowing from the pipette to the cell) are mainly due to anions flowing outwards.

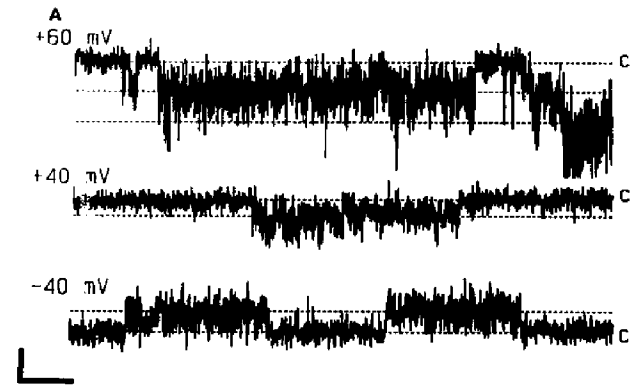

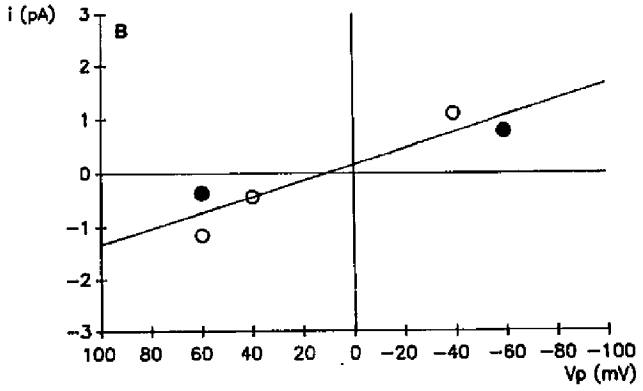

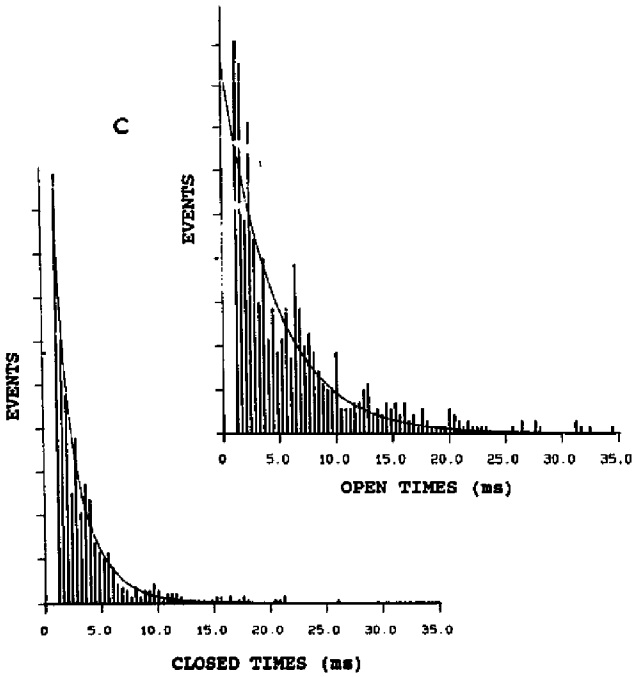

In the cell-attached configuration, the large channel was voltage-dependent, with the time spent in the open state being longer for outward currents than for inward currents (Fig. 4A). Its conductance was 26 pS (3 experiments) and the channel current reversed at $V_r = 4$ mV (Fig. 4B). The channel kinetics was characterized by the transition between at least two closed states and one open state (Fig. 4C).

Ion substitution experiments were performed in the cell-attached configuration to study the selectivity of the large channel (Fig. 4D). Replacing potassium by choline in the pipette had very little effect on either channel conductance or V_r. When chloride in the pipette was replaced by sulfate or aspartate, the channel conductances were reduced to 18 and 16 pS, respectively, and V_r shifted to -26 mV. However, when acetate was substituted for chloride, there was no detectable V_r shift, indicating that this anion is as permeant as chloride in SF-9 cell membranes, a phenomenon for which we have no explanation. Reducing the chloride concentration in the pipette resulted in a progressive shift of V_r towards more negative pipette potentials. These experiments demonstrate that the

Fig. 2. Single-channel currents in SF-9 cells recorded in the cell-attached configuration with normal pipette-filling solution and NBS in the bath. (A) Representative records at three different pipette voltages (indicated next to the traces). The letter C indicates the closed state of the channels. Vertical bar = 1 pA. Horizontal bar = 1s. (B) Current-voltage relation for the same channel (two experiments). The straight line was fitted by linear regression to the data points. Its slope was 15 pS. (C) Open and closed time histograms of the same channel at +40 mV (pipette voltage). The open-time histogram was fitted by one exponential and the closed-time histogram was fitted by two exponentials using a nonlinear regression procedure. The time constants of the exponential functions are the channel's mean open time (t_0) and mean closed times (t_{c1} and t_{c2}). They were: $t_0 = 4.5$ ms, $t_{c1} = 0.8$ ms and $t_{c2} = 2.4$ ms. Vertical scale = 7 events/div (open-time histogram), and 14 event/div (closed-time histogram). Horizontal scale: as indicated on graphs.

large channel is anionic and is mainly selective for chloride ions.

Exposure of the cytoplasmic side of the cell membrane to the toxin was tested in the inside-out configuration with symmetrical solutions (13 experiments). In symmetrical potassium chloride solutions, the appearance of channel activity following toxin exposure had the same time course as that observed in the cell-attached configuration. Although small channels could be seen occasionally, only the large channel was regularly observed. Its conductance and kinetics were similar to those of the large channel observed in the cell-attached configuration. When potassium was replaced by choline, the same large, voltage-dependent channel was observed (Fig. 5A). Its conductance was 18 pS (three experiments; Fig. 5B) and it displayed kinetic properties similar to the 26 pS channel observed in the cell-attached configuration (Fig. 5C).

The selectivity of the large channel in the inside-out configuration was investigated using various concentrations of chloride in the bath. The zero-current membrane potential shifted towards more negative values (i.e. positive pipette voltages) as chloride ions were progressively replaced by aspartate ions (Fig. 5D). A

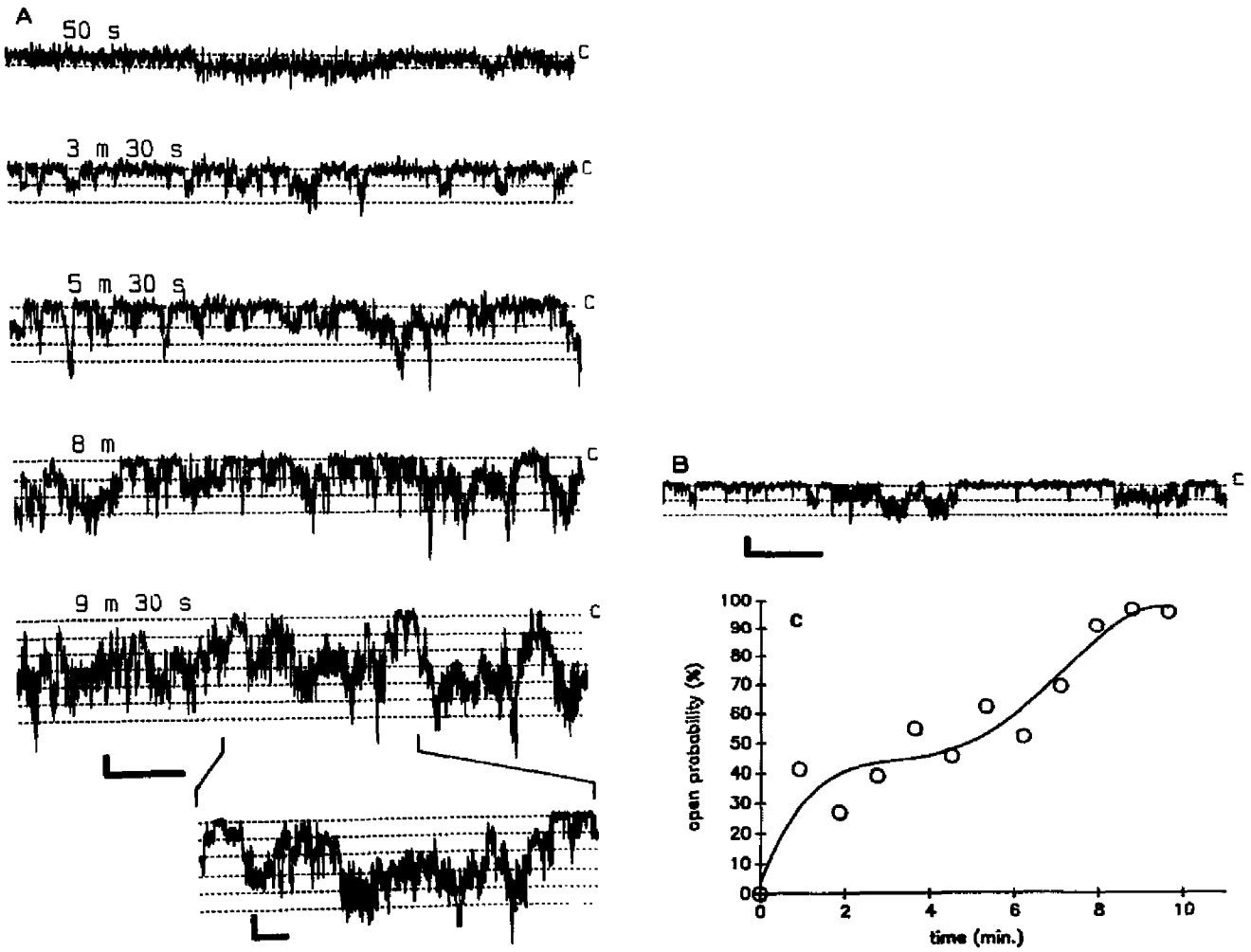

Fig. 3. Effect of δ-endotoxin exposure on SF-9 cells. Cell-attached configuration with NBS in the bath. The toxin was added to the bath at $t = 0$. Pipette voltage was set to +40 mV. (A) Representative channel activity at various times (indicated above each trace) after addition of the toxin. Pipette was filled with the normal pipette-filling solution. The upper trace shows activity of a channel similar to that illustrated in Fig. 2. Note the amplitude of 0.6 pA at $V_p = 40$ mV and the long openings and closures of this channel (several seconds). Larger unitary currents are seen on the five other traces, the last one representing an expanded time scale section of the record at 9 min 30 s. Note that this channel (second and following traces) has an amplitude of about 1 pA and demonstrates faster kinetics than the one shown in the top trace. Vertical bar = 1 pA. Horizontal bar = 1 s (first five traces) and 200 ms (bottom trace). (B) Typical channel activity at $t = 3$ min 30 s with choline replacing potassium in the pipette. (C) Time course of increasing channel activity in response to δ-endotoxin exposure (data from another cell in the same experimental conditions as in Fig. 3A. In this experiment, only large channel activity was observed). The vertical axis represents the percentage of time spent by the large channels in the open state.

Nernst plot of this shift (Fig. 5D, inset) shows that the four points corresponding to the highest concentrations of chloride in the bath could be fitted by a straight line of about 50 mV/decade, indicating that the channel behaves as a chloride electrode.

Discussion

We report, for the first time, single-channel activity in lepidopteran SF-9 cells. We also present the first evidence that, when these cells are exposed to sub-

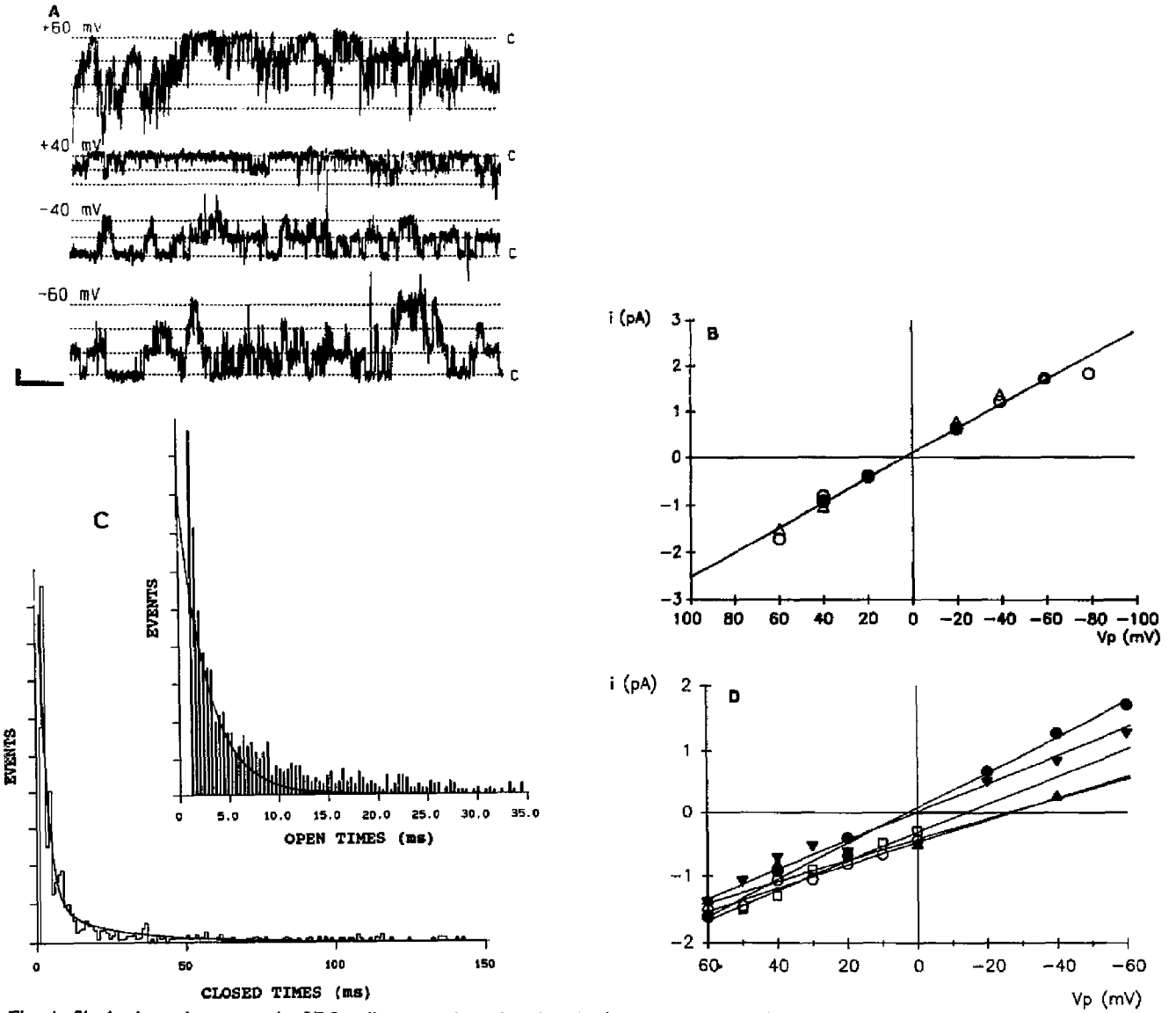

Fig. 4. Single-channel currents in SF-9 cells exposed to δ-endotoxin (added to the bath). Currents were recorded in the cell-attached configuration with normal pipette-filling solution and NBS in the bath. (A) Representative records at four different pipette voltages (indicated next to the traces). Note that the +60 mV record was obtained several minutes later, which explains the higher level of activity of the channels. The letter C indicates the closed state of the channels. Vertical bar = 1 pA. Horizontal bar = 1 s. (B) Current-voltage relation for the same channel (three experiments). The straight line was fitted by linear regression to the data points. Its slope was 26 pS. (C) Open- and closed-time histograms of the same channel at +40 mV (pipette voltage). The open-time histogram was fitted by one exponential and the closed-time histogram was fitted by two exponentials using a nonlinear regression procedure. The time constants of the exponential functions are the channel's mean open time (t_0) and mean closed times (t_{c1} and t_{c2}). They were: $t_0 = 2.9$ ms, $t_{c1} = 2.4$ ms and $t_{c2} = 22.0$ ms. Vertical scale = 11 events/div (open-time histogram), and 16 events/div (closed-time histogram). Horizontal scale: as indicated on graphs. (D) Current-voltage relations for various ionic substitutions in the pipette. Filled circles: 135 mM KCl (26 pS, three experiments); filled downward triangles: 35 mM KCl/100 choline chloride (22 pS, three experiments); open squares: 35 mM KCl/100 potassium aspartate (23 pS, three experiments); open circles: 135 mM potassium sulfate (18 pS, two experiments); filled upward triangles: 135 mM potassium aspartate (16 pS, five experiments). Each data point represents the mean of values obtained in the same experimental conditions. The straight lines were fitted by linear regression to the data points.

lethal doses of either native or recombinant CryIC activated toxin from *Bacillus thuringiensis*, there is an immediate, non-toxic rise in intracellular calcium followed by the activation of anion selective channels mainly permeable to chloride. This was demonstrated by the combined use of single-channel electrophysiological recordings and dual-excitation wavelength microspectrofluorescence of the intracellular calcium probe fura-2.

Cytoplasmic calcium concentration in SF-9 cells in-

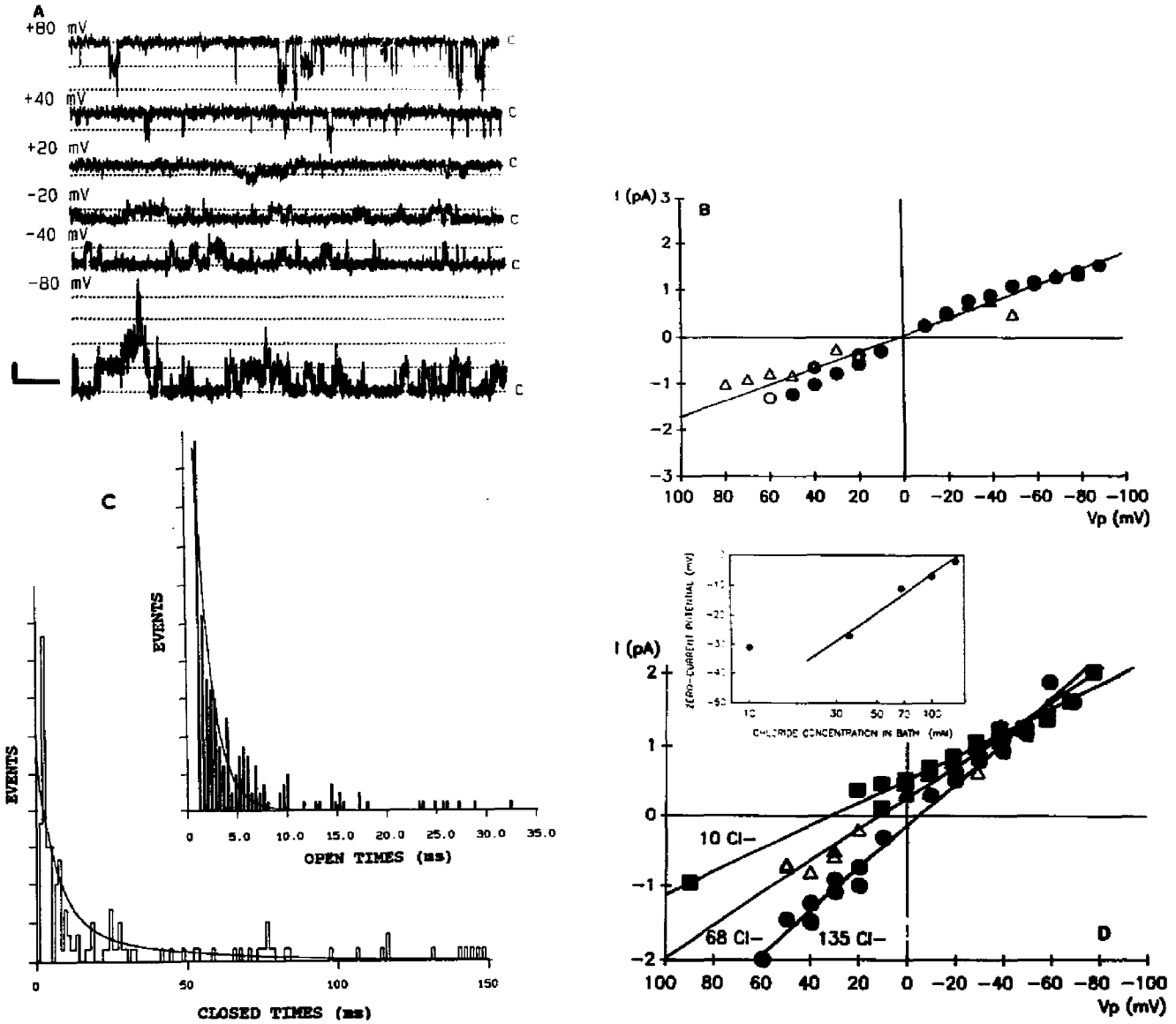

Fig. 5. Single-channel currents recorded from SF-9 cells in the inside-out configuration, in the presence of δ-endotoxin on the cytoplasmic side of the membrane patch. Recordings were performed in symmetrical choline chloride solutions (Figs. 5A, B and C). For Fig. 5D, chloride was isotonically replaced by aspartate as indicated. (A) Representative records at six different pipette voltages (indicated next to the traces). The letter C indicates the closed state of the channels. Vertical bar = 1 pA. Horizontal bar = 1s. (B) Current-voltage relation for the same channel (three experiments). The straight line was fitted by linear regression to the data points. Its slope was 18 pS. (C) Open and closed time histograms of the same channel at +40 mV (pipette voltage). The open-time histogram was fitted by one exponential and the closed-time histogram was fitted by two exponentials using a nonlinear regression procedure. The time constants of the exponential functions are the channel's mean open time (t_0) and mean closed times (t_{c1} and t_{c2}). They were: $t_0 = 1.5$ ms, $t_{c1} = 6.2$ ms and $t_{c2} = 34.2$ ms. Vertical scale = 4 events/div (open-time histogram), and 3 events/div (closed-time histogram). Horizontal scale as indicated on graphs. (D) Current-voltage relation for the same channel with various chloride concentrations in the bath (as indicated on the graph). The straight lines were fitted by linear regression to the data points. Filled circles: 135 mM Cl^- (30 pS, two experiments); open triangles: 68 mM Cl^- (22 pS, two experiments); filled squares: 10 mM Cl^- (16 pS, two experiments). (Inset) Nernst plot of the zero-current membrane voltage (i.e., $-V_p$) versus chloride concentration in the bath, for the same experiments as above and two additional concentrations (35 mM Cl^-, two experiments, and 100 mM Cl^-, two experiments). The four right-most points were fitted by straight line regression (48 mV/decade).

creased when the potassium concentration in the bath was raised to 45 mM. This effect was suppressed in the presence of D-600 or cobalt ions. Therefore, it appears that voltage-dependent calcium channels are present in SF-9 cells and that they activate upon depolarization. A much larger calcium response was observed immediately after toxin treatment at sublethal levels. This intracellular calcium rise was also mainly due to the influx of extracellular calcium through voltage-dependent calcium channels, as demonstrated by the fact that it reversed when calcium was removed outside, or when calcium channel blockers were added to the bath. These experiments, although they provide evidence for the role of calcium channels in the first phase of the detected response of SF-9 cells to δ-endotoxin exposure, do not indicate whether single calcium channel activity is increased, more channels are recruited, or new channels are formed in the plasma membrane by the toxin. In any case, calcium entry through calcium channels is one of the earliest events taking place following exposure to the toxin. This step does not appear to be cytolytic. It could, however, be responsible for the insertion in the cell membrane of larger molecules, including the toxin itself or a toxin-receptor complex [19].

Our patch-clamp experiments revealed the presence of endogenous anionic channels in SF-9 cells. This is the first demonstration of channel activity in these cells which are widely used as a baculovirus expression system [20]. Although whole-cell potassium currents have been recorded in SF-9 cells expressing the Drosophila Shaker potassium channel, there is no report on channel activity in the wild-type cells [21]. These small, 15-pS channels observed in our experiments displayed a low level of activity and tended to run down rapidly. We have no explanation for this phenomenon. However, within minutes following exposure of SF-9 cells to a sublethal dose of δ-endotoxin, progressively increasing activity of a different type of anionic channel of larger conductance took place. These channels, never seen in the absence of the toxin, were mainly permeable to chloride. It is not possible to rule out that this toxin-induced channel activity is not the result of the unmasking of normally silent endogenous channels, the alternative being, of course, the insertion of new channels in the plasma membrane. In any case, it seems that anionic channel activation or insertion constituted the second detectable step of the non-cytolytic action of the toxin, following the initial calcium influx in the cell.

This study provides additional evidence for the concept of ion channel involvement in the mode of action of δ-endotoxin. However, it does not support the K^+-channel hypothesis proposed by Wolfersberger et al. [8], Sacchi et al. [9], Crawford and Harvey [10] and Wolfersberger [11]. These investigators suggest that K^+ channels play a major role in the cytolytic effect of δ-endotoxins. Knowles et al. [12] and Slatin et al. [13] reported the formation by δ-endotoxin of cation-selective channels in planar lipid bilayers. The latter studies were performed on artificial membranes that did not possess the toxin receptors thought to be responsible for the specificity of toxin action. They demonstrated that the toxin can insert itself in lipid bilayers at high pH. Contrary to the reported results, we did not observe potassium-selective channels in cultured SF-9 insect cells. Furthermore, we recorded toxin-dependent channel activity at slightly acidic pH, and the channels involved were mainly anion-selective, with a preference for chloride ions.

It cannot be excluded that the mode of action for CryIC toxins differs from that of other *B. thuringiensis* gene classes characterized to date [3]. However, the number of conserved features seen among the known lepidopteran-specific genes, including the general mechanism of killing, rules against such a hypothesis. Furthermore, an argument has been made that the mode of toxin action on cultured insect cells does not accurately reflect the in vivo situation, since some gene classes, toxic for the insect, do not affect their respective cell line. This is presumably due to lack of specific receptor expression on the non-midgut cultured cell surface rather than altered modes of toxin action. SF-9 cells, when exposed to lethal concentrations of the activated CryIC toxin, rapidly round up followed by cell swelling until lysis occurs (data not shown). The same morphological changes have been recorded for midgut epithelium cells [22] and other cultured cell lines [23].

When exposed to the toxin, SF-9 cells displayed identical channels (the 26-pS channels referred above as the large channels) in the cell-attached configuration and in the inside-out configuration of the patch-clamp technique. This provides additional information about the possible mode(s) of action of the toxin. In the cell-attached configuration, the extracellular side of the membrane patch, being isolated under the patch pipette, is not exposed to the toxin. Therefore, direct coupling between the toxin receptor and the ion channel (through a G-protein or as a receptor-channel complex), or channel formation by the toxin inserting itself from the external side of the membrane can be excluded. Instead, one might consider two other possibilities: either the toxin (or a toxin-receptor complex) activates an intracellular second messenger that in turn recruits endogenous channels in the plasma membrane, including some channels located under the pipette, or the toxin (or a toxin-receptor complex) gets internalized and reinserts itself, from inside, in the cell membrane, including the patch membrane under the pipette.

Examination of toxin-induced channel activity in the

inside-out configuration produced unexpected results. In this configuration, with the toxin in the bath, toxin binding to external surface receptors or mobilization of intracellular messengers are both excluded. The activity seen may be explained by the following: the toxin could activate endogenous channels by binding to specific sites located on the cytoplasmic side of the channel; the toxin could bind to intracellular receptors coupled to existing channels; or finally, the toxin could simply insert itself from underneath the membrane patch and form channels de novo.

We propose the following model to describe the early events of the cytolytic effects of the δ-endotoxin CryIC of *B. thuringiensis* on cultured lepidoteran SF-9 cells. This model is consistent with the generally accepted specificity of the toxin, the early rise in cytosolic calcium observed in our fluorescence experiments and the dual mode of action deduced from our patch-clamp studies, i.e. an indirect mode, through the activation of channels in a membrane patch not directly exposed to the toxin (as is the case in cell-attached experiments), and a direct mode, by activation of channels in a membrane patch whose cytoplasmic side is exposed to the toxin (inside-out experiments).

Initially, the toxin binds to a specific receptor at the surface of the cell. This triggers the immediate activation of calcium channels and the entry of calcium ions in the cell. The resulting sustained, non-toxic rise of intracellular calcium concentration either promotes diffusion in the cytoplasm of the toxin-receptor complex, or facilitates receptor-mediated endocytosis of the toxin. In the case of toxin endocytosis, the following events may take place. First, the increased level of intracellular calcium (or possibly another second messenger) activates native chloride channels in the cell membrane (the 15-pS anionic channels observed shortly after the beginning of toxin exposure). The proton pumps of the toxin-filled vesicles are then stimulated by the entry of chloride ions in the cell. Finally, acidification of the vesicles results in the release of the toxin in the cytosol. In the case of toxin-receptor complex internalization, the toxin separates from its receptor by an unknown mechanism. In both cases, the toxin, now present in the cytosol, either unmasks existing anionic channels (e.g., the 26 pS channel never observed in the absence of the toxin), through direct activation or via a third messenger mechanism, or inserts itself in the plasma membrane and forms chloride-permeable pores.

The gradual increase in anion channel activity and/or the progressive recruitment of new anion channels could then result in obliged water movement and, ultimately, cell lysis through mechanisms similar to those proposed by other investigators [5,7].

In the above scenario, based on our results demonstrating the role of calcium and chloride channels in the early response of SF-9 cells to CryIC δ-endotoxin treatment, we have introduced several mechanisms that are found in various cells exposed to hormones, bacterial toxins or viruses, although there is no evidence for their existence in our cell system. Cell surface receptors for δ-endotoxins have been found in *Choristoneura fumiferana* CF-1 lepideptoran cells [24] and in midgut brush border membranes from *Manduca sexta, Heliothis virescens, Spodoptera littoralis* [25] and *Lymantria dispar* [26]. It is established that, upon ligand binding, receptor-operated calcium channels are gated by G-protein-related mechanisms [27]. Receptor internalization [28] and receptor-mediated toxin endocytosis occur in many cells and for a large variety of ligands, including bacterial toxins [29]. There are several indications that acidification of endocytic vesicles might result in toxin-receptor dissociation and toxin penetration from the vesicles to the cytoplasm [30]. Low pH can promote the entry of toxins through the plasma membrane, as has been shown for diphtheria toxin [31]. Large channels formed by botulinum, tetanus, and diphtheria toxins are pH-gated and display pH-dependent conductance and selectivity, being cationic at alkaline pH and anionic at acidic pH [32]. In fact, preliminary experiments in our laboratory show that the anionic channels observed in response to exposure of SF-9 cells to CryIC δ-endotoxin at pH 6.4 may indeed be selectively permeable to cations at pH 9. Finally, it has been suggested that a membrane-permeant anion is needed for the vesicle proton pump to achieve acidification [33] and that an influx of Ca^{2+} in the cell is required for toxin internalization [19].

In summary, the present study demonstrates the primary role of ion channels in the early response of cultured lepidopteran SF-9 cells exposed to CryIC δ-endotoxin from *B. thuringiensis*. More specifically, it shows that, at an early stage following toxin treatment, rapid recruitment of calcium channels takes place, free intracellular calcium concentration rises, and within minutes, increasing numbers of anion channels become activated. Our model could be used as a working hypothesis for further research in the elucidation of the mode of action of insecticidal proteins from *B. thuringiensis*.

Acknowledgements

We thank D. Thomas and J.F. Whitfield for their interest in this work and valuable comments. The assistance of M. Caron, A. Mazza and G.A.R. Mealing is gratefully acknowledged. The HPLC-purified CryIC toxin isolated from *B. thuringiensis* var. *entomocidus* crystal was a kind gift from M. Pusztai, Institute for Biological Sciences, NRC, Ottawa.

References

1 Aronson, A.I., Beckman, W. and Dunn, P. (1986) Microbiol. Rev. 50, 1–24.
2 Brousseau, R. and Masson, L. (1988) Biotechnol. Adv. 6, 697–724.
3 Höfte, H. and Whiteley, H.R. (1989) Microbiol. Rev. 53, 242–255.
4 Davidson, E.W. (1989) in Advances in Cell Culture (Maramorosh, K., ed.), Vol. 7, pp. 125–146, Academic Press, New York.
5 Knowles, B.H. and Ellar, D.J. (1987) Biochim. Biophys. Acta 924, 509–518.
6 Himeno, M. (1987) J. Toxicol.-Toxin Rev. 6, 45–71.
7 English, L.H. and Cantley, L.C. (1985) J. Membr. Biol. 85, 199–204.
8 Wolfersberger, M.G., Hofmann, C. and Lüthy, P. (1986) Zentralbl Bakt. Mikrobiol. Hyg. Suppl. 15, 237–238.
9 Sacchi, V.F., Parenti, P., Hanozet, G.M., Goirdana, B., Luther, P. and Wolfersberger, M.G. (1986) FEBS Lett. 204, 213–218.
10 Crawford, D.N. and Harvey, W.R. (1988) J. Exp. Biol. 137, 277–286.
11 Wolfersberger, M.G. (1989) Arch. Insect Biochem. Physiol. 12, 267–277.
12 Knowles, B.H., Blatt, M.R., Tester, M., Hersnell, J.M., Carroll, J., Menestrina, G. and Ellar, D.J. (1989) FEBS Lett. 244, 259–262.
13 Slatin, S.L., Abrams, C.K. and English, L. (1990) Biochem. Biophys. Res. Commun. 169, 765–772.
14 Hamill, O.P., Marty, A., Neher, E., Sakmann, B. and Sigworth, S.J. (1981) Pflügers Arch. (Eur. J. Physiol.) 391, 85–100.
15 Tsien, R.Y., Rink, T.J. and Poenie, M. (1985) Cell Calcium 6, 145–157.
16 Masson, L., Préfontaine, G., Peloquin, L., Lau, P.C.K. and Brousseau, R. (1989) Biochem. J. 269, 507–512.
17 Bradford, M.M. (1976) Anal. Biochem. 72, 248–254.
18 Grynkiewicz, G., Poenie, M. and Tsien, R.Y. (1985) J. Biol. Chem. 260, 3440–3450.
19 Olsnes, S. and Sandvig, K. (1985) in Endocytosis (Pastan, I. and Willingham, M.C., eds.), pp. 195–234, Plenum Press, New York.
20 Miller, L.K. (1988) Annu. Rev. Microbiol. 42, 177–179.
21 Klaiber, K., Williams, N., Roberts, T.M., Papazian, D.M., Jan, L.Y. and Miller, C. (1990) Neuron 5, 221–226.
22 Lüthy, P. and Ebersold, H.R. (1981) in Pathogenesis of invertebrate microbial diseases (Davidson, E.W., ed.), pp. 235–267, Allanheld, Osmun Publishers, Totowa, NJ.
23 Percy, J. and Fast, P.G. (1983) J. Invert. Pathol. 41, 86–98.
24 Knowles, B.H. and Ellar, D.J. (1986) J. Cell Sci. 83, 89–101.
25 Van Rie, J., Jansens, S., Höfte, H., Degheele, D. and Van Mellaert, H. (1990) Appl. Environ. Microbiol. 56, 1378–1385.
26 Wolfersberger, M.G. (1990) Experientia 46, 475–478.
27 Birnbaumer, L., Abramowitz, J. and Brown, A.M. (1990) Biochim. Biophys. Acta 1031, 163–224.
28 Hollenberg, M.D. (1986) Experientia 42, 718–727.
29 Pastan, I. and Willingham, M.C. (1985) in Endocytosis (Pastan, I. and Willingham, M.C., eds.), pp. 1–44, Plenum Press, New York.
30 Maxfield, F.R. (1985) in Endocytosis (Pastan, I. and Willingham, M.C., eds.), pp. 235–257, Plenum Press, New York.
31 Sandvig, K. and Olsnes, S. (1981) J. Biol. Chem. 256, 9068–9076.
32 Hoch, D.H. and Finkelstein, A. (1985) Ann. N.Y. Acad. Sci. 456, 33–35.
33 Ohkuma, S., Moriyami, Y. and Takano, T. (1982) Proc. Natl. Acad. Sci. USA 79, 2758–2762.